JOURNAL OF NATURAL PRODUCTS

pubs.acs.org/jnp

Article

Insight into the Interaction of *Humulus lupulus* L. Specialized Metabolites and Gastrointestinal Bitter Taste Receptors: *In Vitro* Study in STC-1 Cells and Molecular Docking

Ludovica Lela,[▽] Maria Ponticelli,[▽] Vittorio Carlucci, Jan F. Stevens, Immacolata Faraone, Nikolay T. Tzvetkov,* and Luigi Milella*

Cite This: *J. Nat. Prod.* 2024, 87, 2021−2033

Read Online

ACCESS | Metrics & More | Article Recommendations | Supporting Information

ABSTRACT: Bitter taste receptors, also known as taste 2 receptors (T2R), are expressed throughout the body and are involved in regulating different physiological processes. T2R expression in the intestinal tract regulates orexigenic and anorexigenic peptide secretion, thus becoming potential a potential target for controlling food intake and the prevalence of obesity and overweight. The present study aims to investigate the implication of hop bitter compounds such as α-acids, β-acids, and xanthohumol in the secretion of anorexigenic hormones and T2R expression in intestinal STC-1 cells. The tested bitter compounds induced the secretion of the anorexigenic hormones glucagon-like peptide 1 and cholecystokinin concurrently with a selective increase of murine *Tas2r* expression. Xanthohumol and α-acids selectively increase *Tas2r*138 and *Tas2r*130−*Tas2r*138 expression, respectively, in STC-1 cells, while β-acids increased the expression of all bitter receptors studied, including *Tas2r*119, *Tas2r*105, *Tas2r*138, *Tas2r*120, and *Tas2r*130. Increased intracellular calcium levels confirmed this activity. As all investigated bitter molecules increased *Tas2r*138 expression, computational studies were performed on *Tas2r*138 and its human orthologue T2R38 for the first time. Molecular docking experiments showed that all molecules might be able to bind both bitter receptors, providing an excellent basis for applying hop bitter molecules as lead compounds to further design gastrointestinal-permeable T2R agonists.

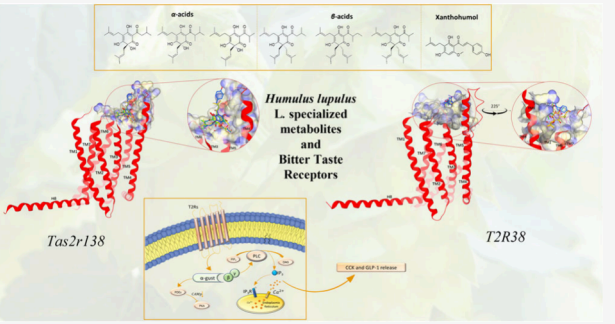

INTRODUCTION

The sensation of bitterness, detected on the tongue, represents an important physiological defense mechanism, providing information about ingesting potentially harmful/toxic substances rather than healthy ones. The responsibility for bitter taste perception is attributed to G protein-coupled receptors (GPCRs) belonging to the family of taste type 2 receptors designated as T2R and *Tas2r* for human and mouse receptors, respectively.[1] Although bitter receptors are primarily associated with taste sensation in the oral cavity, in recent years, numerous studies have shown that these receptors are also expressed in other tissues such as the skin, lungs, reproductive system, and gastrointestinal tract.[2] Considering that taste perception is not required in this extra-oral tissue, it has been long believed that bitter receptors located in these body compartments might be involved in other physiological processes.[2] Recent investigations have, indeed, demonstrated the association of these bitter taste receptors with the regulation of processes like bronchial relaxation, inflammation, or enteroendocrine system control.[2] Despite their different distributions, it seems that either oral or extraoral bitter receptors have the same morphology and mechanism of action. Specifically, in gastrointestinal enteroendocrine cells (EECs), their activation by bitter substances lead to the secretion of hormones implicated in the modulation of gastrointestinal tract functions such as metabolic homeostasis and hunger regulation.[3,4] Based on the gastrointestinal region involved, the release of different enterohormones may be modulated after the activation of T2R. The most important ones are ghrelin, glucagon-like peptide 1 (GLP-1), cholecystokinin (CCK), and peptide YY (PYY),[2] with some of them primarily affecting the vagus nerve, leading to the regulation of satiety and gastrointestinal tract mobility.[5] Therefore, they represent potential therapeutic targets for preventing obesity and overweight. With this scope, we decided to investigate bitter taste molecules of *Humulus lupulus* L. as promising candidates for preventing or treating overweight and obesity.[6] *H. lupulus* bitter acids, called α-acids (humulones) and β-acids

Received: May 7, 2024
Revised: July 30, 2024
Accepted: July 30, 2024
Published: August 10, 2024

https://doi.org/10.1021/acs.jnatprod.4c00532
J. Nat. Prod. 2024, 87, 2021−2033

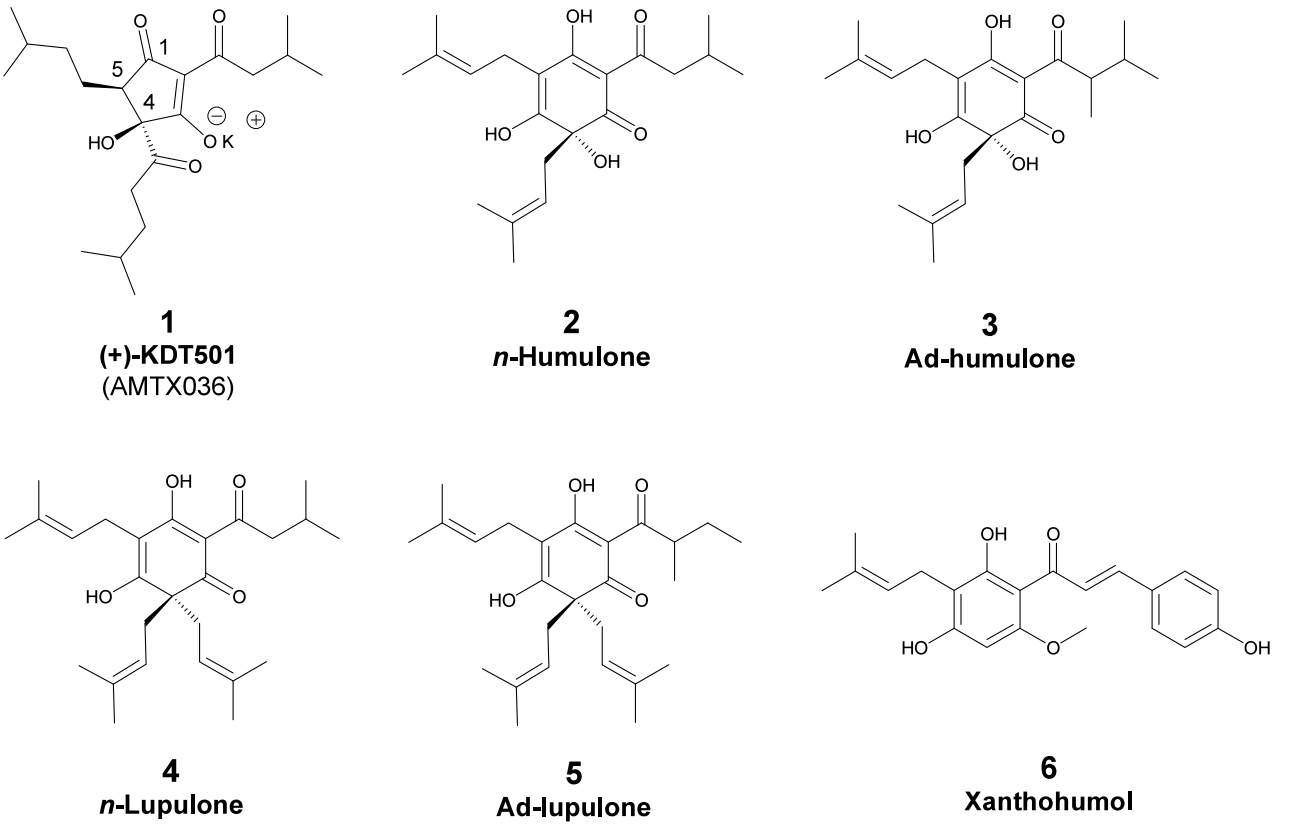

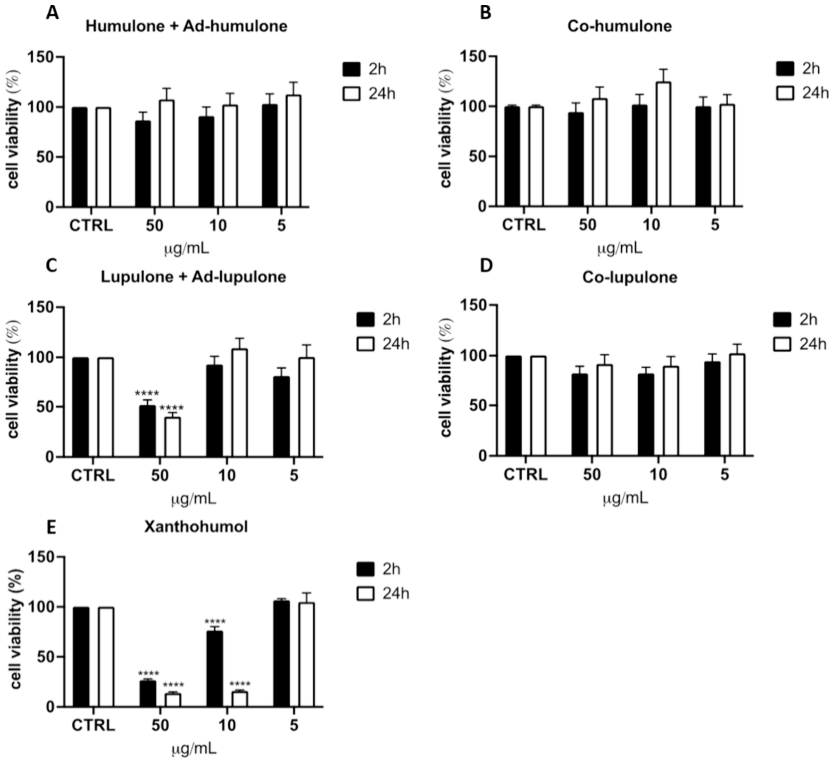

Figure 1. Cell viability evaluated by MTT assay of STC-1 cells treated with different concentrations (50−10−5.0 μg/mL) of (A) humulone + ad-humulone, (B) co-humulone, (C) lupulone + ad-lupulone, (D) co-lupulone, and (E) xanthohumol. Data are expressed as the mean ± SD of three independent experiments (n = 3). One-way ANOVA and Dunnett's multiple comparison test: ****p < 0.0001 vs control (CTRL).

(lupulones), and prenylflavonoids, such as xanthohumol, are chemical compounds found in hop flowers conferring bitterness, aroma, and flavor to beer.[7] Only a few investigations have focused on recognizing T2R using hop-bitter molecules, demonstrating that such bitter compounds are involved in activating bitter taste type 2 receptors T2R1, T2R10, T2R14, T2R40, and T2R46.[8,9] On the other hand, a compound chemically derived from hop extracts, designated as KDT501,

https://doi.org/10.1021/acs.jnatprod.4c00532
J. Nat. Prod. 2024, 87, 2021−2033

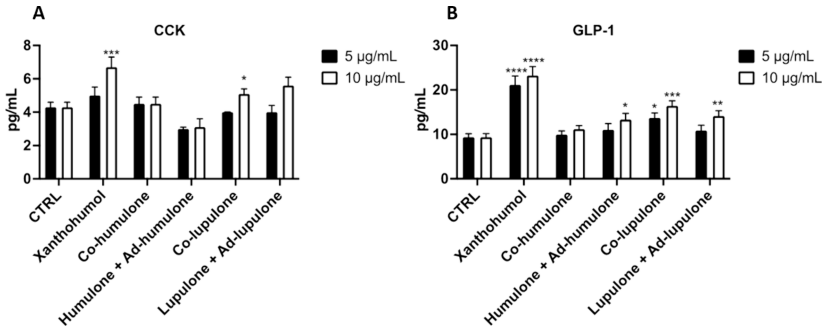

Figure 2. Effect of hop bitter compounds on (A) CCK and (B) GLP-1 secretion in STC-1 cells. Xanthohumol, the β-acids, and humulone + ad-humulone fraction II significantly increased the secretion of GLP-1 hormone, while xanthohumol and lupulone + ad-lupulone fraction IV (10 μg/mL) increased the secretion of CCK after 120 min of treatment of STC-1 cells. Data are displayed as the mean ± SD of three independent experiments (n = 3). One-way ANOVA and Dunnett's multiple comparison test: ****p < 0.0001, ***p < 0.001, **p < 0.01, and *p < 0.05 vs untreated cells (CTRL).

was demonstrated to possess antidiabetic and antiobesity properties through activation of mouse intestinal bitter taste receptor *Tas2r*108.[10] However, as far as we know, only one study investigated the *in vitro* interaction of hop bitter compounds with T2R using a HEK293 cell-based TAS2R system, while no study has been performed on STC-1 cells. For this reason, the present study aims to investigate the effect of hop α-acids (humulone, ad-humulone, and co-humulone), β-acids (lupulone, ad-lupulone, and co-lupulone), and xanthohumol standard bitter compound on anorexigenic hormone secretion and bitter taste receptor expression using intestinal STC-1 cells as a model system. More specifically, herein, the ability of hop bitter compounds to increase the expression of five different receptors known to be expressed in the intestinal tract was investigated, including the mouse intestinal bitter taste receptors *Tas2r*119, *Tas2r*105, *Tas2r*138, *Tas2r*120, and *Tas2r*130, whose human receptor orthologs are T2R1, T2R10, T2R38, T2R46, and T2R7, respectively.[2] Finally, molecular modeling experiments were performed, including homology modeling and subsequent docking studies, to predict the binding modes and affinity of all investigated hop bitter compounds toward mouse and human bitter taste receptors *Tas2r*138 and T2R38, respectively.

RESULTS AND DISCUSSION

Purification of Hop Pure Compounds from ICE-4 by Semipreparative HPLC-DAD and Structure Elucidation by UHPLC-MS/MS. Semipreparative HPLC was applied to obtain pure sample fractions from the ICE-4 standard mixture. Figure S1 reports the chromatogram showing all collected fractions (FRs). Each peak (1−4) was collected in three subfractions (ascending, apex, and descending parts), resulting in 156 subfractions after 14 injections at a concentration of 100 mg/mL. All fractions obtained were analyzed by UHPLC-MS/MS and compared with the UV spectra and mass fragmentation patterns from the literature, which allowed us to reunite fractions with an identical content of hop bitter acids and to obtain four final fractions as follows: FR I co-humulone (77.43 mg), FR II humulone + ad-humulone (106.45 mg), co-lupulone FR III (11.71 mg), and lupulone + ad-lupulone FR IV (18.98 mg). The hop bitter acids or mixtures (e.g., fractions II and IV) identified in fractions I−IV are reported in Table S1. Due to their similar chemical properties and identical retention time (t_R), it was not possible to separate the n- from the ad-forms of either α- or β-acids. In addition, the appropriate UV and MS/MS spectra of the separated fractions I−IV are shown in Table S2.

Cell Viability. The viability of STC-1 cells was assessed by MTT assay to test the toxicity of *H. lupulus* pure bitter compounds (co-humulone, co-lupulone, and xanthohumol) and fractions II (humulone + ad-humulone) and IV (lupulone + ad-lupulone). As shown in Figure 1, the α-acids co-humulone and humulone + ad-humulone did not reduce the viability of STC-1 cells after 2 and 24 h incubation periods (Figure 1A and B). However, β-acids, particularly lupulone + ad-lupulone, showed marked cytotoxicity at the highest tested concentration of 50 μg/mL, reducing the cell viability by 60% after 24 h of treatment (IC_{50} = 44.5 ± 2.12 μg/mL) (Figure 1D). Xanthohumol also showed notable toxicity at the same concentration (50 μg/mL), reaching an IC_{50} of 35.3 ± 3.40 μg/mL at 2 h and that of 8.00 ± 0.65 μg/mL at 24 h (Figure 1E). At a concentration of 10 μg/mL, xanthohumol reduced cell viability by approximately 35% after 24 h of treatment, which agrees with its general anticancer activity. At the lowest concentrations of 5 and 10 μg/mL, none of the tested α- and β-acids, including fractions FR II and FR IV, inhibited cell viability. Based on the data obtained, even if, in some cases, a reduced metabolic activity is found, the cells do not show signs of suffering or morphological alterations upon microscopic analysis. Therefore, subsequent experiments were conducted using treatments at concentrations of 5 and 10 μg/mL for 2 h.

Hop Bitter Compounds Stimulate Gut Hormone Secretion. Taking into consideration that the enteroendocrine cells secrete hormones involved in inducing the sense of satiety or hunger and the promising activity linked to bitter substances, we decided to investigate whether hop compounds, including xanthohumol and α- and β-acids, can modulate the secretion of GLP-1 and CCK. As reported in Figure 2A, xanthohumol statistically increased the secretion of GLP-1 in a dose-dependent manner with an almost 2-fold increase in activity compared to the control (untreated) cells. For xanthohumol, the measured values were 20.39 ± 1.95 and 28.39 ± 2.00 pg/mL at 5.0 and 10 μg/mL, respectively, compared to 13.29 ± 1.30 pg/mL for the control cells (Figure 2A). Furthermore, the humulone + ad-humulone and all β-acids (co-lupulone and lupulone + ad-lupulone) induced GLP-1 release from the cells, especially at a concentration of 10 μg/mL. In contrast , co-humulone did not influence GLP-1 secretion at either 5 or 10 μg/mL.

https://doi.org/10.1021/acs.jnatprod.4c00532
J. Nat. Prod. 2024, 87, 2021−2033

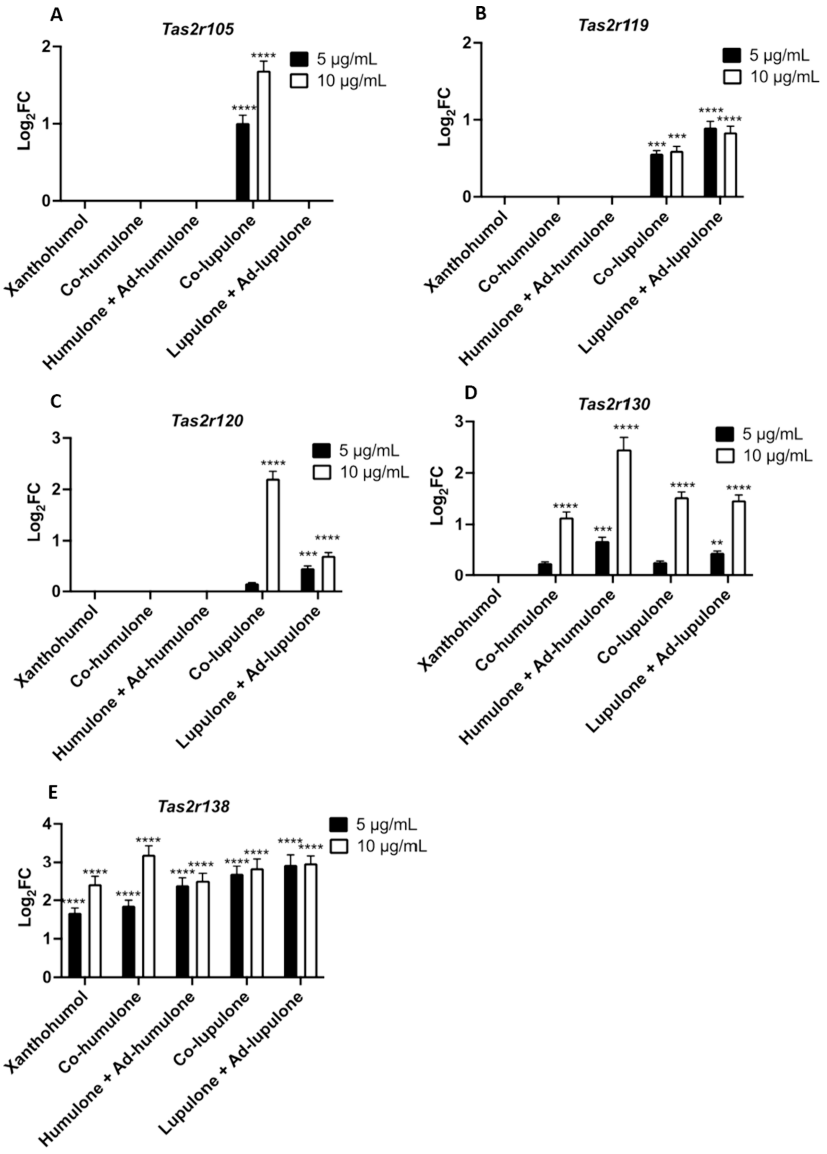

Figure 3. Effects of pure *H. lupulus* compounds on gene expression. Co-lupulone and lupulone + ad-lupulone significantly induce the expression of the bitter receptors (A) *Tas2r*105, (B) *Tas2r*119, (C) *Tas2r*120, (D) *Tas2r*130, and (E) *Tas2r*138. The α-acids co-humulone and humulone + ad-humulone upregulated *Tas2r*130 and, together with xanthohumol, *Tas2r*138. Data are normalized with the housekeeping gene polymerase II (Pol II) and are shown as Log_2 fold change treated/control ± standard deviation (SD) of three independent experiments ($n = 3$). One-way ANOVA and Dunnett's multiple comparison test: **** $p < 0.0001$, *** $p < 0.001$, ** $p < 0.01$ vs control.

Regarding CCK secretion, only xanthohumol and β-acids (co-lupulone and lupulone + ad-lupulone) influenced CCK release compared to the control at the highest tested concentration of 10 μg/mL (Figure 2B).

The results obtained corroborate those found in the literature, since matured hop extract was demonstrated to stimulate the secretion of CCK and GLP-1 in STC-1 cells.[11] This activity may be related to the reduction in hunger, fat mass, and body weight and improvement in glucose homeostasis observed in rodents and humans after hop extract administration.[12] A recent investigation indeed showed that humans' assumption of hop bitter extract suppressed the *ad libitum* energy intake, an effect accompanied by an increase in plasma levels of GLP-1 and CCK.[13] Therefore, the present investigation demonstrated for the first time that the observed activity of the hop extracts may primarily be attributed to xanthohumol and β-acids, as they are implicated in the increase in either GLP-1 or CCK.

Bitter Receptor Gene Expression Profiling. STC-1 cells were treated with reference xanthohumol and α- or β-acids (fractions I and IV) to identify their mechanism of action in inducing hormone secretion. As expected, the compounds demonstrated different behaviors in increasing the expression of the considered bitter receptors (Figure 3). More precisely, the β-acids increase the expression of all studied receptors, showing particular activity on mouse bitter taste receptors *Tas2r*105 (co-lupulone, Figure 3A), *Tas2r*119 and *Tas2r*120 (co-lupulone and lupulone + ad-lupulone, Figure 3B and C), and *Tas2r*138 (all tested compounds, Figure 3E). On the other hand, α-acids upregulated only *Tas2r*138 and *Tas2r*130, whereas xanthohumol increased only the expression of *Tas2r*138 with a comparable effect compared to all other tested compounds (Figure 3D and E). It should be mentioned

https://doi.org/10.1021/acs.jnatprod.4c00532
J. Nat. Prod. 2024, 87, 2021−2033

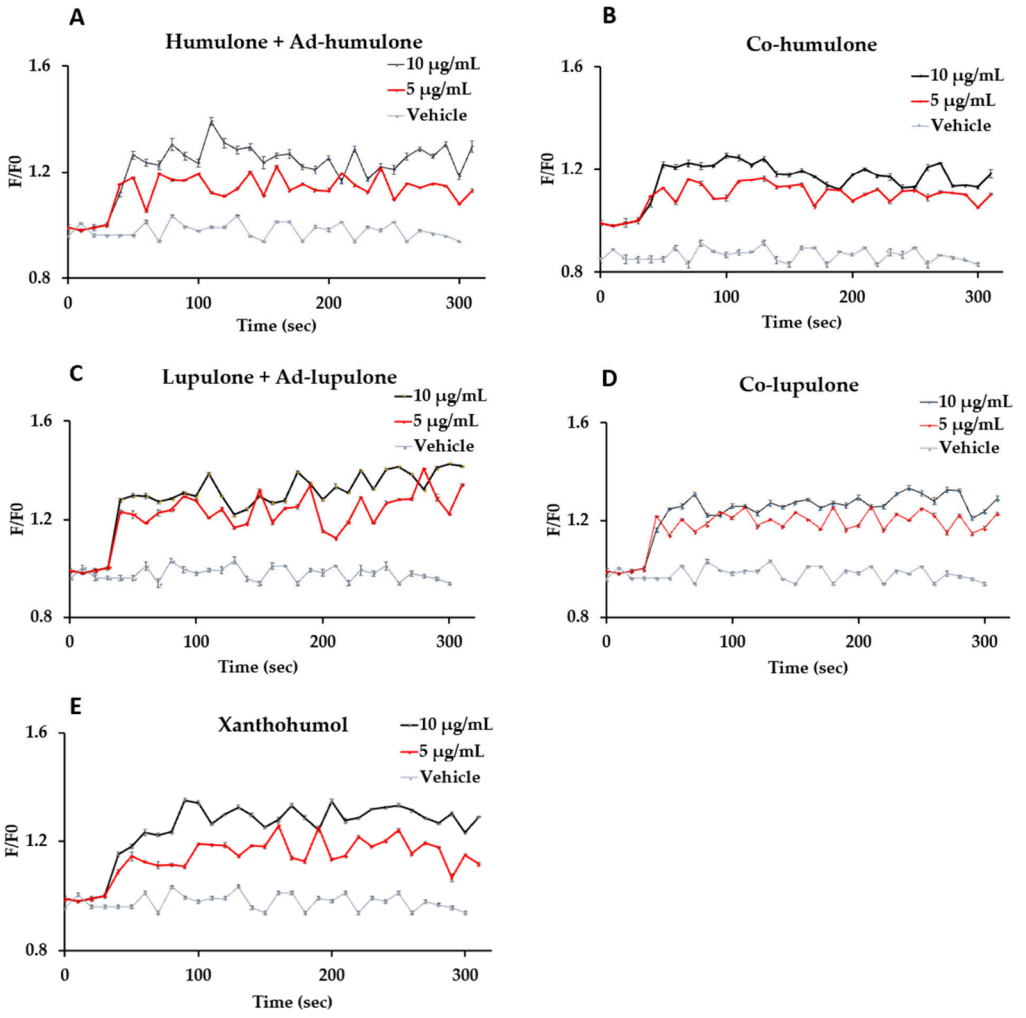

Figure 4. Hop bitter pure compounds rapidly increased intracellular [Ca^{2+}] ([Ca^{2+}]$_i$) dose-dependently in STC-1 cells. Cells were loaded with 5 μM calcium indicator dye Fluo 4-AM for 30 min at 37 °C in the dark, and fluorescence was recorded every 10 s for 5 min. Results are expressed as F/F0, where F0 is the baseline fluorescence.

that the activity of all tested α- or β-acids against *Tas2r*120 and *Tas2r*130, but not *Tas2r*119, was more pronounced at 10 ppm than at 5.0 μg/mL.

The results obtained are relevant, since it was demonstrated that hop-bitter compounds could selectively modulate the expression of *Tas2r*. In this regard, a representative example is the reference xanthohumol and α-acids, which were found to significantly increase the expression of *Tas2r*138 (xanthohumol) and *Tas2r*130−*Tas2r*138 (α-acids) in STC-1 cells. Moreover, all of the investigated molecules can enhance the expression of *Tas2r*138. This finding is highly interesting in relation to the human ortholog T2R38, whose polymorphism might be associated with the development of obesity,[14] as it is linked to food preferences, nutrition, diet, and efficient immune response.[15] Therefore, selectively targeting T2R38, as indirectly suggested by *in vitro* studies herein, could greatly benefit the treatment of obesity and related disorders.

Increase in Hop Bitter Compounds ([Ca^{2+}]i) in STC-1 cells. As is well-known, an assessment of when and how much a gene is expressed can be made by measuring the functional activity of a gene product. When bitter taste components or some amino acids bind T2R, GPCRs are activated, triggering second messenger synthesis, including cAMP and IP3, and resulting in Ca^{2+} release from intracellular depots.[16] Therefore, to demonstrate the evaluated increased expression of T2R by hop bitter pure compounds, the effect of these molecules on enhancing Ca^{2+} levels in enteroendocrine cells was also evaluated. Within this scope, the cell-permeant Ca^{2+}-sensitive dye Fluo-4-AM was used. As shown in Figure 4, all tested compounds increased calcium concentrations dose-dependently. In particular, β-acids induced a slightly higher increase in intracellular Ca^{2+} levels than α-acids, especially the fraction composed of lupulone + ad-lupulone (Figure 4D). Xanthohumol also affected calcium levels, especially at the highest tested concentration of 10 μg/mL (Figure 4E).

The trend of bitter compounds to increase calcium levels agrees with their capacity to enhance T2R expression, as lupulone + ad-lupulone (fraction IV) exhibits the highest activity in increasing the expression of T2Rs and intracellular Ca^{2+} concentration. The data obtained in this study are supported by a previous investigation demonstrating that an extract of matured hop bitter acids likewise increased calcium levels in STC-1 cells in a dose-dependent manner.[11] Furthermore, another study on HEK-293T cells transiently expressing human bitter receptors also demonstrated the ability of hop molecules to increase the intracellular Ca^{2+} concentration.[9] These findings demonstrated that hop bitter specialized metabolites are able to not only increase the

https://doi.org/10.1021/acs.jnatprod.4c00532
J. Nat. Prod. 2024, 87, 2021−2033

Table 1. Estimated Thermodynamic Binding Values (in kJ/mol) and Binding Affinities ($K_{i,HYDE}$ Ranges) for Humulone, Ad-humulone, Co-humulone, Xanthohumol, Lupulone, Ad-lupulone, and Co-lupulone[c]

		Lupulone	Ad-lupulone	Co-lupulone	Humulone	Ad-humulone	Co-humulone	Xanthohumol
Tas2r138	$K_{i\,HYDE}$ (μM)	0.02–1.92	0.04–3.62	0.09–8.93	0.19–19.3	0.78–77.3	0.78 –77.5	7.10–706
	$\overline{K}_{i\,HYDE}$ (μM) [a]	0.97	1.83	4.51	9.75	39.0	39.1	~356
	pK_i [b]	7.713	7.438	7.047	6.712	6.109	6.108	5.149
	ΔG	–38.05	–36.49	–34.23	–32.34	–28.94	–28.77	–23.49
	–TΔS	–19.23	–17.66	–15.42	–14.25	–11.65	13.00	–10.10
	ΔH	–18.83	–18.83	–18.82	–18.09	–17.29	–41.77	–13.39
	Torsions	O	O	O	O	O	O	O
	Inter-clashes	O	O	O	O	O	O	O
	Intra-clashes	O	O	O	O	O	O	O
		Ad-humulone	Co-lupulone	Lupulone	Ad-lupulone	Xanthohumol	Humulone	Co-humulone
T2R38	$K_{i\,HYDE}$ (μM)	0.58–58.1	3.04–302	5.37–534	7.77–772	8.62–856	13.2–1312	30.7-3051
	$\overline{K}_{i\,HYDE}$ (μM) [a]	29.3	~153	~270	~390	~433	~663	~1540
	pK_i [b]	6.233	4.513	5.270	5.110	5.065	4.879	4.513
	ΔG	–29.15	–25.44	–24.04	–23.11	–22.86	–21.90	–19.26
	–TΔS	43.09	11.55	10.32	13.77	15.77	24.19	45.23
	ΔH	–72.249	–36.99	–34.36	–36.88	–38.63	–46.09	–64.49
	Torsions	O	O	O	O	O	O	O
	Inter-clashes	O	O	O	O	O	O	O
	Intra-clashes	O	O	O	O	O	O	O

[a] $\overline{K}_{i,HYDE}$ = predicted median $K_{i,HYDE}$ values obtained from the respective $K_{i,HYDE}$ ranges (both in μM). [b] pK_i is related to the lower value of $K_{i,HYDE}$ (μM). [c] HYDE coloring scheme for the most important docking parameters, including torsional, inter- (ligand-receptor amino acid), and intramolecular clashes (within the ligand), was always "green" meaning "good for affinity".

expression of the selected intestinal bitter receptors but also induce their activation.

Homology Modeling of *Tas2r*138 and Comparison with T2R38. Considering the data obtained from the *in vitro* experiments, we decided to make a prediction of the possible interactions of all investigated hop bitter compounds with mouse bitter taste receptor *Tas2r*138 and its human orthologue T2R38 by molecular modeling computations, including homology modeling and molecular docking. A detailed examination of the potential binding modes of all hop bitter compounds revealing the most significant interactions within the ligand–receptor binding site might provide useful information for (i) the observed preference in selectivity against *Tas2r*138 of α- versus β-acid hop bitter compounds in comparison with xanthohumol and (ii) the main structural features determining their future applications as selective T2R38 agonists. The molecular modeling experiments represent the first *in silico* study performed so far on both bitter taste receptors *Tas2r*138 and T2R38.

At first, the homology model of the mouse bitter receptor *Tas2r*138 was generated from its amino acid sequence comprising 331 aa residues with a sequence identity of 87.61% (*Tas2r*138 ID output Q4VHE7.1.A) as described in the materials and methods in the Supporting Information (Molecular Modeling section). Next, the PDB structure of T2R38 was obtained from the AlphaFold protein structure database and used for molecular docking experiments without further structural optimizations (T2R38 ID entry P59533-F1).[17] Using PyMol and UGENE software for 3D and 2D comparison, respectively, structural alignment of the homology model of *Tas2r*138 with the 3D structure of T2R38 was performed (Figure S2). Multiple alignment of both receptors was required to identify the common structural (conformational) features of their binding sites, with particular emphasis on the extracellular area of both receptors. It was estimated that the homology models of *Tas2r*138 and T2R38 showed about 66% amino acid sequence identity (*cf.* Figure S2). Examination of the superpositioned 3D structures of *Tas2r*138 (red helices) and T2R38 (blue helices) revealed their similar arrangement within the extracellular part of both receptors and, thus, similarity in the formation of the ligand-binding cavity inside the likewise binding modes (Figure S2A).

Using SeeSAR, the binding site for bitter taste receptors *Tas2r*138 and T2R38 was determined from their respective 3D models. Based on the performed homology modeling, it was found that the binding site of T*as2r*138 (Q4VHE7.1.A) is formed by 37 aa residues, while that of the human bitter taste receptor T2R38 (P59533-F1) is formed by 31 aa residues (Table S3).

Molecular Docking of Hop Bitter Compounds. Docking experiments were performed with both mouse and human bitter taste receptors *Tas2r*138 and T2R38, respectively. The best docking poses for each compound into the binding site of *Tas2r*138 and T2R38 were selected based on their HYDE-estimated binding affinities, as previously described.[18] All docking computations were carried out using the SeeSAR software package (ver. 13.0.4).[19] The ligand–receptor interactions of humulone, ad-humulone, co-humulone, lupulone, ad-lupulone, co-lupulone, and xanthohumol within the binding pockets of *Tas2r*138 and T2R38 are listed in Table S4.

Considering the best-computed docking solutions in accordance with HYDE-estimated binding affinities ($K_{i,HYDE}$ ranges), it was possible to hypothesize that the most virtually active compounds on *Tas2r*138 may be lupulone and ad-lupulone (Table 1). The predicted main contribution to the binding affinity of lupulone is due to the carbon atom C23 (HYDE − 4.2 kJ/mol) involved in an alkyl interaction with PRO87, a π–alkyl interaction with HIS90, and van der Waals interactions with LEU88 (Figure 5A). Similarly, the predicted main contribution to the binding affinity of ad-lupulone is due to C23 (HYDE − 3.9 kJ/mol), which is also involved in an

https://doi.org/10.1021/acs.jnatprod.4c00532
J. Nat. Prod. 2024, 87, 2021−2033

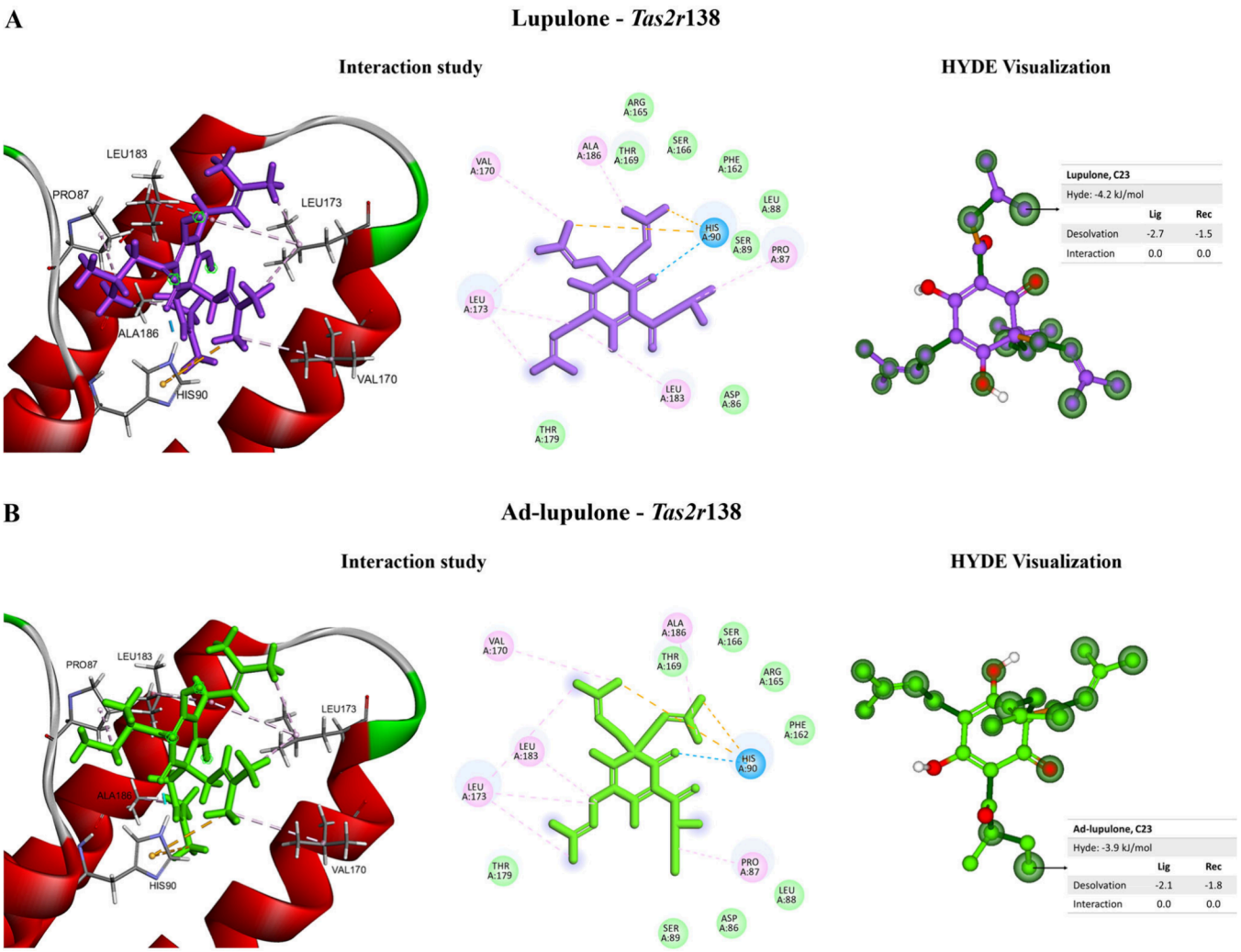

Figure 5. 3D (left) and 2D representations (middle) of the interaction of (A) lupulone and (b) ad-lupulone with the binding pocket of *Tas2r*138 (Q4VHE7.1.A)created using Biovia Discovery Studio 2021.[20] Color 2D interaction scheme: green = van der Waals, light blue = hydrogen bonds, dark blue = carbon hydrogen bond, pink = alkyl, orange = π−alkyl. SeeSAR ver. 13.0.4 was used to perform and visualize the HYDE assessment (right). HYDE coloring scheme: green = favorable and red = unfavorable for the overall free energy of binding (ΔG in kJ/mol).

alkyl interaction with PRO87 and van der Waals interactions with residues ASP86 and LEU88 (Figure 5B). The predicted binding interactions within the best-scored binding modes for all other molecules are shown in Supporting Information Figure S3A−E.

Regarding the human receptor T2R38, the most virtually active compound was estimated to be ad-humulone (0.58 μM < $K_{i,\mathrm{HYDE}}$ < 58.1 μM), followed by co-lupulone (3.04 μM < $K_{i,\mathrm{HYDE}}$ < 302 μM) (*cf.* Table 1). The predicted main contribution to the binding affinity of ad-humulone is due to the oxygen atom O1 (HYDE = 6.1 kJ/mol) involved in hydrogen bond interactions with amino acid residues ILE274 and ARG274, an alkyl interaction with ARG274, and van der Waals interactions with LEU272 (Figure 6A). Concerning co-lupulone, the main contribution to the binding affinity is due to C28 (HYDE = 4.2 kJ/mol) involved in an alkyl interaction with PRO87 and van der Waals interactions with GLU86 (Figure 6B). The binding interactions within the best-scored binding modes for all other molecules are visualized in Supporting Information Figure S4A−E.

In summary, based on all docking solutions computed with SeeSAR, it is possible to assume that the ligands may occupy the same binding cavity within the respective receptor *Tas2r*138 or T2R38. Due to the structural similarity of the individual compounds within the investigated α-acids and β-acids series, the simulated binding modes resulted in similar conformations, and their best-scored binding poses show the same orientation for the respective ligand within the "ligand cavity".

HYDE Visual Free Energy Assessment and Computed Thermodynamic Profiling. The implemented SeeSAR HYDE algorithm was used to predict the possible binding affinity of hop bitter molecules for *Tas2r*138 and T2R38. The thermodynamic profiles, including the Gibbs free energy (ΔG), the enthalpic (ΔH) and entropic ($-T\Delta S$) terms, and the HYDE-estimated binding affinity ($K_{i,\mathrm{HYDE}}$ ranges) obtained from the best-scored docking poses for all ligands (humulone, ad-humulone, co-humulone, lupulone, ad-lupulone, co-lupulone, and xanthohumol) on *Tas2r*138 and T2R38 are reported in Figure S5 and Table 1. Based on the HYDE visual affinity assessment, agreement between the $K_{i,\mathrm{HYDE}}$ ranges and the overall binding affinity (ΔG values) could be observed for all ligands toward both bitter receptors (from mid to low μM

https://doi.org/10.1021/acs.jnatprod.4c00532
J. Nat. Prod. 2024, 87, 2021−2033

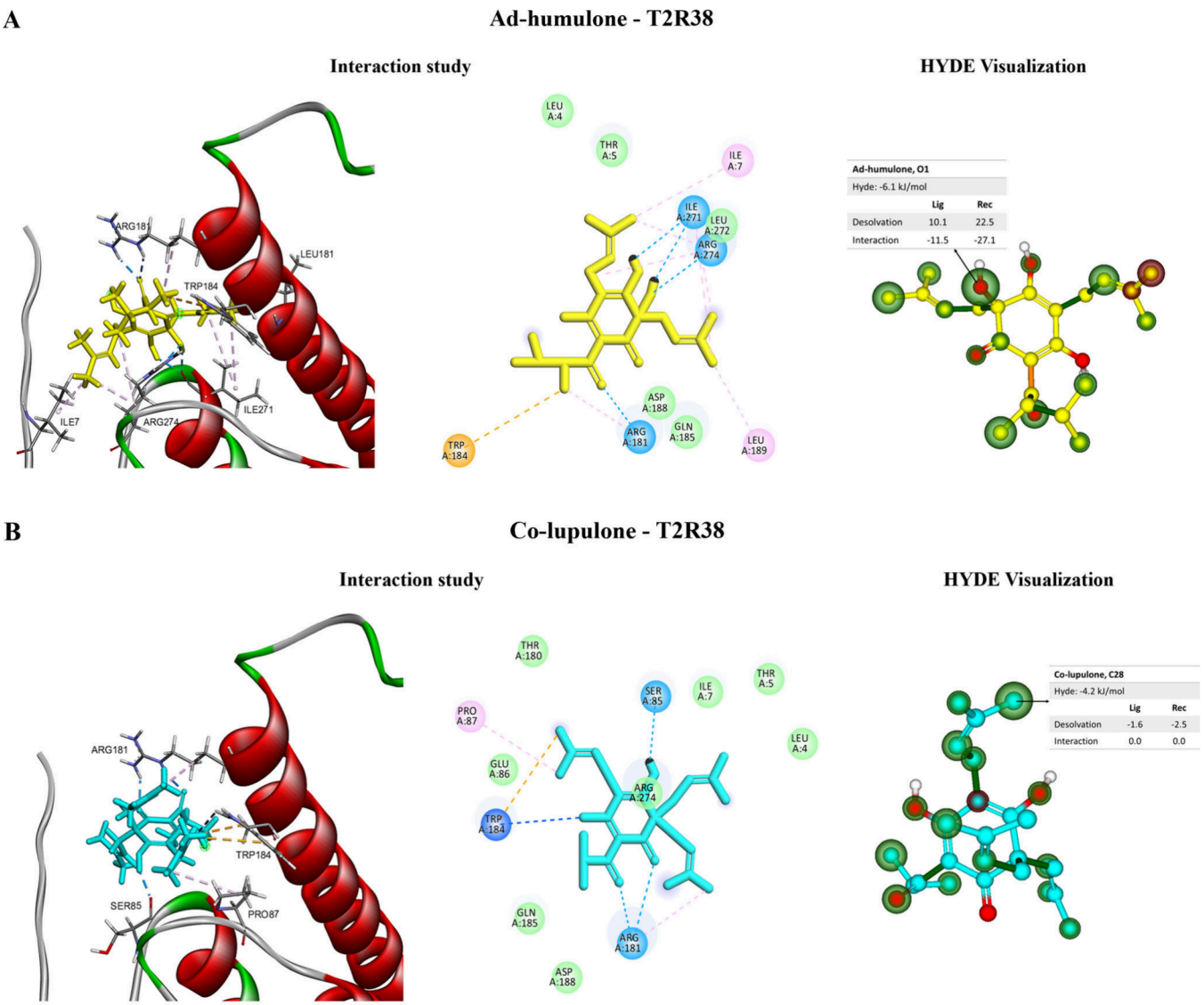

Figure 6. 3D (left) and 2D representations (middle) of the interaction of (A) ad-humulone and (b) co-lupulone with the binding pocket of T2R38 (P59533-F1) created using Biovia Discovery Studio 2024.[20] Color 2D interaction scheme: green = van der Waals, light blue = hydrogen bonds, dark blue = carbon hydrogen bond, pink = alkyl, orange = π−alkyl, violet = π−cation, magenta = π−π stacked. SeeSAR ver. 13.0.4 was used to perform and visualize the HYDE assessment (right). HYDE coloring scheme: green = favorable and red = unfavorable for the overall free energy of binding (ΔG in kJ/mol).

ranges), as the lowest $\bar{K}_{i,\mathrm{HYDE}}$ always corresponded to the lowest (negative) ΔG value (*cf.* Table 1).

As reported in Table 1, the predicted $K_{i,\mathrm{HYDE}}$ ranges indicated higher affinities for all hop bitter compounds at mouse *Tas2r*138 than at human bitter receptor T2R38. In particular, this means that a greater concentration of hop bitter compounds should be required to activate human receptor T2R38. The most virtually active compound against T2R38 is ad-humulone, followed by co-lupulone, while for the mouse *Tas2r*138 the β-acids (lupulone, ad-lupulone, and co-lupulone) are the most active compounds, thus confirming *in vitro* experiments. The obtained activity order indeed corresponds to the increased expression of *Tas2r*138 observed at the lowest concentration of 5.0 μg/mL tested on STC-1 cells. The differences in affinities for mouse *Tas2r*138 versus human T2R38 can also be explained by the different contributions to the overall binding affinity, since in the case of *Tas2r*138 binding is due to both hydrogen bond (ΔH) and desolvation (dehydration) interactions, while in the case of T2R38 the thermodynamic profile of all bitter compounds showed a predominant enthalpic contribution to the overall Gibbs binding energy (ΔG) (*cf.* Figure S5). The observed disparities can be primarily related to differences in the orthosteric binding pocket. In the case of *Tas2r*138, the active site is included in the extracellular part of transmembrane helices TM3, TM4, and TM5, while for T2R38 the orthosteric binding occurs in the extracellular region of the receptor, comprising of TM1, TM2, TM3, TM5, TM6, and TM7 (Figure 7).

Evaluation of Drug-Likeness. Based on the predicted binding affinities between the hop molecules and both bitter receptors, the relevant physicochemical and drug-like properties of α-acids, β-acids, and xanthohumol were subsequently estimated to evaluate their potential implication in developing new antiobesity drugs (Table 2). These calculated parameters included hydrogen bond acceptor and donor (HBD/HBA)

https://doi.org/10.1021/acs.jnatprod.4c00532
J. Nat. Prod. 2024, 87, 2021−2033

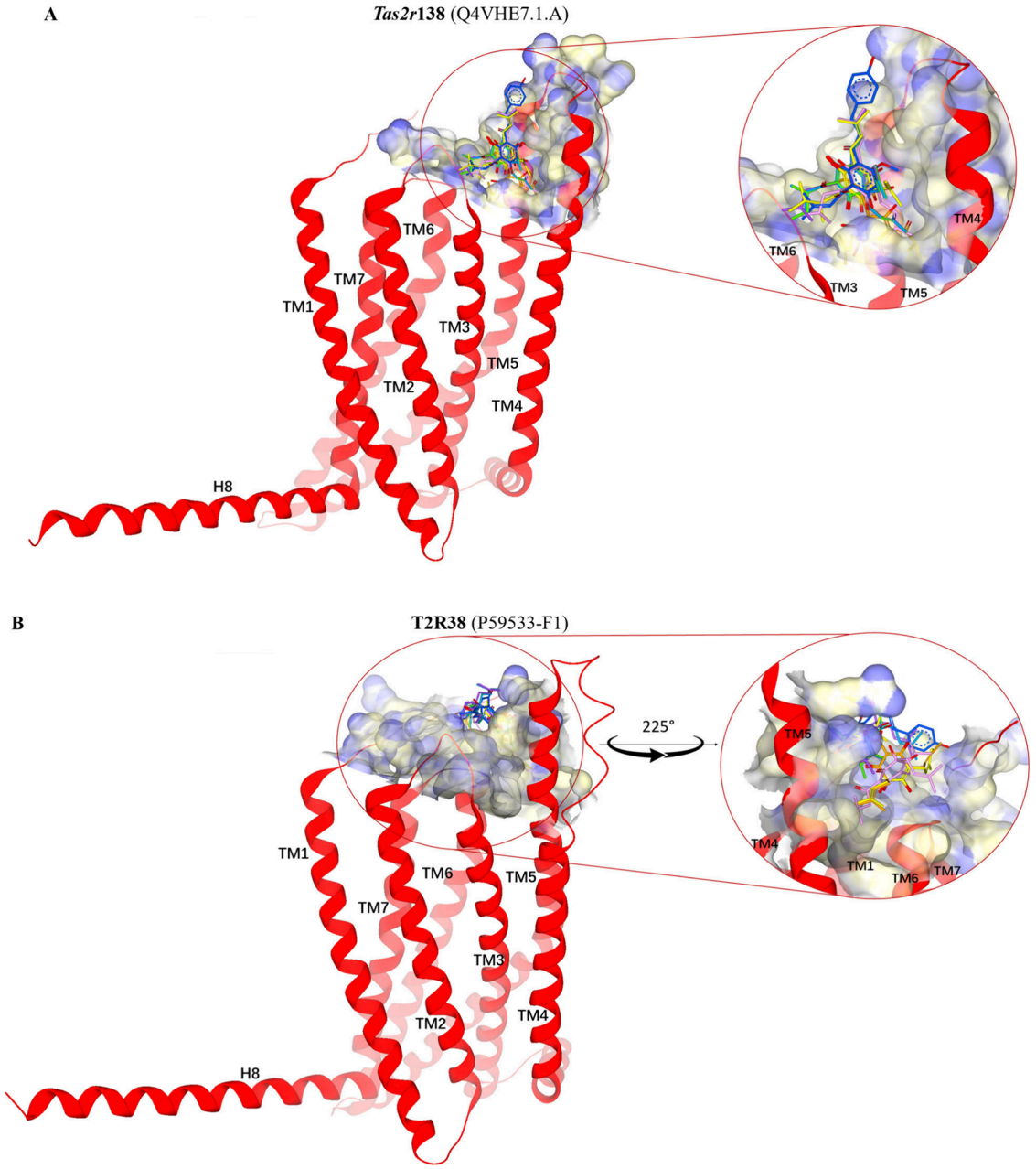

Figure 7. 3D representation of (A) *Tas2r*138 (Q4VHE7.1.A) and (B) T2R38 (P59533-F1) and superposition of ligands as docked within the binding pockets. The transmembrane helices TM1−TM7 are indicated. The binding pockets are shown as a transparent lipophilic−hydrophilic protein surface. The respective ligands are colored as follows: lupulone = violet, co-lupulone = light blue, ad-lupulone = green, humulone = pink, co-humulone = orange, ad-humulone = yellow, and xanthohumol = blue. Molecular docking and visualization were performed using SeeSAR ver. 13.0.4.

counts,[21] number of rotatable bonds (n-RotB),[21] topological polar surface area (tPSA),[22] percent of absorption (% ABS),[23] octanol−water partition and distribution coefficients at pH 7.4 (clogP and clog$D_{7.4}$, respectively), aqueous solubility at pH 7.4 (expressed as clog$S_{7.4}$), and ligand lipophilicity efficiency (LLE).[24,25] The calculated relevant parameters for drug-likeness and all hop bitter compounds are in the suggested limits for oral bioavailability and gastrointestinal absorption and in accordance with Lipinski's rule-of-5 (for drug-like compounds: MW ≤ 500, HBA ≤ 7, HBD ≤ 3, n-RotB ≤ 10, tPSA = 60−140 Å^2, and clogP < 5) (*cf.* Table 2).[26] All investigated bitter compounds have a molecular weight lower than 500, which is very important for their further development as orally applicable drugs. The percentage absorption (% ABS) is a parameter generally used for predicting oral bioavailability, which can be calculated from the topological polar surface area (tPSA, in Å^2). The frequently used parameter tPSA offers a valuable understanding of ligand−receptor interactions and pertinent biological structures involving proteins, particularly concerning hydrogen bonding.[22] TPSA is characterized by the collective surface area (in Å^2) encompassing all polar atoms or molecules, chiefly oxygen and nitrogen, along with their associated hydrogen atoms.[14] It is commonly employed in forecasting cellular absorption, with an optimal tPSA ranging typically between 60 and 140 Å^2.[27] In the case of hop bitter molecules, tPSA ranges between 87.0 and

https://doi.org/10.1021/acs.jnatprod.4c00532
J. Nat. Prod. 2024, 87, 2021−2033

Table 2. Physicochemical and Drug-Like Properties of Hop Compounds

	MW	HBA/D[a]	n-RotB[a]	tPSA[b]	% ABS[c]	clogD$_{7.4}$[b]	clogP[b]	clogS$_{7.4}$[a,d]	LLE[b,e]
humulone	362.46	5:3	7	94.8	76.29	0.601	2.870	−3.20	4.2719
ad-humulone	376.49	4:2	7	94.8	76.29	0.799	3.151	−3.36	4.044
co-humulone	348.44	4:2	6	94.8	76.29	0.455	2.605	−2.93	4.736
lupulone	414.58	4:2	9	74.6	83.26	1.79	4.12	−4.53	1.35
ad-lupulone	414.58	5:3	9	74.6	83.26	1.75	4.17	−4.53	1.34
co-lupulone	400.56	5:3	8	74.6	83.26	1.68	3.90	−4.26	1.81
xanthohumol	354.40	5:3	6	87.0	78.99	3.784	3.784	−3.91	4.0711
Ro5[f]	≤500	≤7:≤3	≤10	60−140	≥60	0−3	<5	≥−5.0	>5

[a]MW, molecular weigth (in Da); HBA/D, number of hydrogen bond acceptor/donors; n-RotB, number of rotatable bonds; tPSA, topological surface area (in Å^2); logBB, blood(plasma)−brain partition coefficient. Predicted using DataWarrior ver. 5.5.0.[30] [b]Estimated using the StarDrop module in SeeSAR ver. 13.0.4.[19] [c]% ABS, percent of absorption = 109 − [0.345 × tPSA].[28] [d]cloS7.4, calculated water solubility in mol/L at pH = 7.5 (25 °C). [e]LLE, ligand-lipophilicity efficiency = pIC$_{50}$ − logP. [f]Rule-of-5.[21,22,31,32]

94.8 Å^2, indicating good bioavailability.[22] Hence, this value was used to evaluate % ABS, obtaining values between 76.29% (for all α-acids) and 83.26% (for all β-acids), along with a value of approximately 79% for xanthohumol. In general, the % ABS for an orally bioavailable drug is higher than or equal to 60%, thus confirming that all investigated compounds are assumed to be orally bioavailable.[22] The number of rotatable bonds for all investigated hop bitter compounds is ≤10, being in the range 6−9 (*cf.* Table 2). It is, in fact, known that a molecule's flexibility and adaptability for efficient interaction with a specific binding pocket increases with the increasing number of rotatable bonds.[28] Furthermore, according to Lipinsky's rule-of-5 for good oral and intestinal absorption, a drug to be administered orally should have a logP value lower than 5 (logP < 5).[26] In the case of the present investigation, the selected compounds have clogP values between 2.6 and 3.8. Other parameters affecting a drug's pharmacokinetics and pharmacodynamics are the water solubility (clogS$_{7.4}$) and distribution coefficients (clogD$_{7.4}$). The calculated logS$_{7.4}$ and logD$_{7.4}$ values for all investigated hop molecules are in the optimal range (logD$_{7.4}$ = 0−3 and logS$_{7.4}$ ≥ −5.0).[29] Altogether, these results support the possibility of using hop bitter compounds to prepare pharmaceutical formulations for oral use as activators (modulators) of T2Rs that are expressed throughout the body.

CONCLUSION

The growing prevalence of obese and overweight people has shifted research toward the study of alternative therapies, often represented by plant species. In recent decades, new targets have been identified for treating obesity and its associated pathologies: extraoral bitter taste receptors. Their expression in other districts, such as the gastrointestinal tract, is involved in numerous functions, such as reducing blood sugar or food intake, thanks to the increased secretion of incretins. Hop inflorescences represent a rich source of specialized bitter metabolites that are not only used for beer production but also exhibit various biological properties in the STC-1 cell line. The present work demonstrates for the first time that hop bitter compounds, such as α-acids, β-acids, and xanthohumol, can stimulate the secretion of the anorexigenic hormones GLP-1 and CCK following a specific increase in murine *Tas2r* expression. Xanthohumol and α-acids selectively enhance the expression of *Tas2r*138 and *Tas2r*130−T*as2r*138, respectively. Meanwhile, β-acids enhance the expression of all tested bitter receptors, including *Tas2r*119, *Tas2r*105, *Tas2r*138, *Tas2r*120, and *Tas2r*130. This effect was further validated by observing increased intracellular calcium levels. Given that all investigated bitter molecules could increase *Tas2r*138 expression, molecular modeling and docking studies were conducted on *Tas2r*138 and its human ortholog T2R38 for the first time. Based on these computational investigations, it was possible to hypothesize that all molecules might be able to bind to the active sites of both bitter receptors with varying affinities. Lupulone and co-lupulone were shown to be the most active on *Tas2r*138, while ad-humulone and co-lupulone were the most active on human T2R38. These findings, supported by further drug-like profiling, suggest the potential of hop bitter molecules as lead compounds for designing novel gastrointestinally active T2R agonists for treating diseases requiring body weight control.

EXPERIMENTAL SECTION

General Experimental Procedures. Xanthohumol (XN) was purchased from Sigma-Aldrich, and the bitter acid mixture standard (internationally calibrated extract, ICE-4) was purchased from the American Society of Brewing Chemists (St. Paul, USA). ICE-4 is a hop extract containing defined amounts of α- and β-acids as follows: co-humulone (13.88%), n-humulone + ad-humulone (30.76%), co-lupulone (13.44%), and n-lupulone + ad-lupulone (10.84%). HPLC-grade water (18 mΩ) was prepared using a Mill-Ω purification system (Millipore Corp., Bedford, MA, USA), and analytical-grade MeOH and H_3PO_4 were purchased from Merck (Darmstadt, Germany and Mollet del Vallés, Spain). The HPLC-DAD system (Shimadzu LC-20AB, Prominence Diode Array Detector, Shimadzu Corporation, Japan) was equipped with a binary pump. A Vanquish UHPLC (Thermo Fisher Scientific Inc., Waltham, MA, USA) was coupled with a DAD and Orbitrap Exploris 120 mass spectrometer system. SPECTROstar^{Nano} (BMG Labtech GmbH, Ortenberg, Germany) was used as the UV−vis spectrometer. The StepOnePlus Real-Time PCR system (Applied Biosystems) was purchased from Thermo Fisher Scientific Inc. (Waltham, MA, USA). Fluo 4-AM and Pluronic F-127 systems were purchased from Thermo Fisher Scientific Inc. (Waltham, MA, USA). The Varioskan TM Flash Multimode Reader was purchased from Thermo Fisher Scientific Inc. (Waltham, MA, USA). Columns were Ascentis C18 (250 × 10 mm, particle size 10 μm) and Phenomenex Luna Omega C18 (100 × 2.1 mm, particle size 1.6 μm) columns. Dulbecco's Modified Eagle Medium (DMEM), trypsin-EDTA solution, glutamine, phosphate saline buffer (PBS), penicillin-streptomycin, and fetal bovine serum (FBS) were purchased from Euroclone (Milan, Italy).

Semi-Preparative Fractionation of ICE-4 Standard. Semi-preparative RP18 HPLC-DAD separations were performed using a reverse phase system (Shimadzu LC-20AB, Prominence Diode Array Detector, Shimadzu Corporation, Japan) equipped with a binary pump. The column was an Ascentis C18 (250 × 10 mm, particle size 10 μm) column operated using two different mobile phases: eluent A (MeOH/H_2O/H_3PO_4, 75:24:1) and eluent B (MeOH). A gradient

https://doi.org/10.1021/acs.jnatprod.4c00532
J. Nat. Prod. 2024, 87, 2021−2033

separation was used as follows: 5 min (50% B), 10 min (50−100% B), 20 min (100% B), 25 min (50% B), 30 min (50% B). The ICE-4 standard was dissolved in MeOH at 100 mg/mL, and 100 μL was injected at a flow rate of 4.0 mL/min. The system was allowed to equilibrate for approximately 10 min for the subsequent injection. Detection was performed by a photodiode array (PDA), and chromatograms were extracted at 325 nm. The standard mix was injected 13 times to obtain an optimal quantity of the individual purified compounds. After semipreparative separation, the obtained fractions were subjected to analytical RP18 HPLC-DAD using the same gradient method as for their separation with a flow rate of 1.0 mL/min and a Macherey-Nagel C18 column (250 × 4.6 mm, particle size 5 μm).

Structure Elucidation by UHPLC/MS. The obtained fractions were further screened by a Vanquish UHPLC (Thermo Fisher Scientific Inc., Waltham, MA, USA) coupled with a DAD and Orbitrap Exploris 120 Mass Spectrometer system to assess the correct fractionation mode. The Orbitrap was coupled to a universal ion source, a heated electrospray ionization (HESI-II) probe. The mass spectra were recorded in negative ion mode $[M - H]^-$. The UHPLC analysis was performed using a Phenomenex Luna Omega C18 column (100 × 2.1 mm, particle size 1.6 μm) with a 5.0 μL injection volume, and each sample was injected into an automatic sampler at 6 °C using two mobile phases: eluent A ($MeOH/H_2O/HCOOH$, 75:24.9:0.1) and eluent B (MeOH). The UHPLC elution was carried out using a mobile phase with a flow rate of 0.2 mL/min and gradient conditions as follows: 5 min (50% B), 10 min (50−100% B), 20 min (100% B), 25 min (50% B). The Orbitrap Fusion Lumos Tribrid MS analysis was performed using constant parameters with a sheath gas flow rate of 10 mL/min, static spray voltage, and capillary temperature of 320 °C during the measurements.

Cell Line and Culture Conditions. The intestinal STC-1 cells were cultured in Dulbecco's Modified Eagle Medium (DMEM) supplemented with 10% fetal bovine serum (FBS), streptomycin (100 μg/mL), penicillin (100 units/mL), and 2 mM glutamine and maintained in a humidified atmosphere with 5% CO_2 at 37 °C. All selected standard compounds were dissolved in DMSO and diluted to the tested concentrations with fresh medium immediately prior to testing. DMSO-treated cells (0.8%, v/v) were used as the control (CTRL) throughout the experiments. Cells were grown to 70−80% confluence before further use in the experiments.

Cell Viability Assay of Pure Compounds and Fractions. The MTT assay was used to evaluate the cell viability on STC-1 cells. Cells were seeded in a 96-well plate (1.5×10^4 cells/well), incubated overnight, and treated with three different concentrations of xanthohumol, co-humulone, n-humulone + ad-humulone, co-lupulone, and n-lupulone + ad-lupulone, (5−10−50 μg/mL) for 2 and 24 h. After removal of the medium, the cells were incubated with 0.75 mg/mL of the MTT solution in PBS for 4 h. Then, the solution was removed, and the cells were solubilized using a DMSO/isopropanol (1:1) solution. The solubilized purple formazan originating from the reduction of the yellow tetrazolium salt (IUPAC name: 3-(4,5-dimethylthiazol-2-yl)-2,5-diphenyltetrazolium bromide, MTT) by succinate dehydrogenase of the viable cells was spectrophotometrically quantified at 560 nm using a UV−Vis spectrophotometer (SPECTROstar^{Nano}; BMG Labtech GmbH, Ortenberg, Germany).

Glucagon-Like Peptide 1 (GLP-1) and Cholecystokinin (CCK) Secretion Assay Mediated by Xanthohumol and α- and β-Acids. STC-1 cells (2×10^5 cells/well) were seeded into 12-well plates for 48 h. The cells were washed three times with PBS and incubated for 120 min with 5 and 10 μg/mL pure compounds or fractions. At the end of the treatment, the medium was collected and centrifuged at 12 000*g* for 5 min to remove the cellular debris. Supernatants were stored at −80 °C until analyses. GLP-1 secretion was evaluated by using a GLP-1 multispecies ELISA kit (Invitrogen BMS2194), while CCK secretion was evaluated by applying a CCK EIA kit (Sigma-Aldrich RAB0039), both purchased from Thermo Fisher Scientific Inc. (Waltham, MA, USA) and used according to the manufacturer's protocol.

Quantitative RT-PCR. Prior to the treatment, STC-1 cells were seeded into 6-well plates and incubated for 48 h, after which the cells were treated for 2 h with 5 and 10 μg/mL xanthohumol and α- and β-acids. After treatment, RNA was isolated by using a specific kit (Qiagen GmbH, Hilden, Germany) and stored at −80 °C until further analysis. The concentration and purity of the RNA was measured using a Nanodrop Lite Spectrophotometer (Thermo Fisher Scientific Inc., Waltham, MA, USA). All PCR primers were purchased from Integrated DNA Technologies, Inc. (IDT; Coralville, IA, USA). Using Primer-BLAST software, the PCR primers were designed toward the *Mus musculus* sequences, available from the NCBI GenBank sequence database. All primer sequences are listed in Table S5. For the real-time quantitative polymerase chain reaction (real-time qPCR), RNA samples were reverse transcribed using the high-capacity cDNA reverse transcription kit (Applied Biosystems, Thermo Fisher Scientific Inc., Waltham, MA, USA). The cDNA amplification was performed by real-time PCR on a StepOnePlus Real-Time PCR System (Applied Biosystems, Thermo Fisher Scientific Inc., Waltham, MA, USA) using an iTAQ Universal SYBR Green supermix kit (Bio-Rad Laboratories Inc., Hercules, CA, USA). To ensure the quality of the amplification product, melt curve analysis was performed as a final step. Samples were tested in triplicate (n = 3), and the gene expression was normalized to levels of polymerase-II. The comparative threshold cycle method (ΔΔCt) was used to quantify the relative amounts of product transcripts.

Intracellular Calcium Measurement. Intracellular calcium was measured in 96-well black plates. Briefly, STC-1 cells (1.5×10^4 cells/well) were seeded. After 48 h, cell-permeant Ca^{2+}-sensitive fluorescent dye Fluo-4-AM (5.0 μM) together with the nonionic copolymer surfactant Pluronic F-127 was loaded into the cells for 30 min at 37 °C using PBS. Fluorescence measurements were performed at an excitation of 490 nm and an emission wavelength of 516 nm using a microplate reader Varioskan TM Flash Multimode Reader (Thermo Fisher Scientific Inc., Waltham, MA, USA). The baseline was recorded before the injection of the bitter compounds at each tested concentration (5−10 μg/mL). The fluorescence was recorded every 10 s for a period of 5 min in accordance with the literature.[33] The measured peak responses were normalized relative to the background florescence, and the results are expressed as F/F0, where F0 is the baseline fluorescence.

Statistical Analysis. Data were expressed as the mean ± standard deviation (mean ± SD). Statistical analysis was performed using GraphPad Prism 8.0 Software Inc. (San Diego, CA, USA), and p-values ≤0.05 were considered statistically significant.

Molecular Modeling. Molecular modeling experiments were performed to validate the experimental data from *in vitro* investigations on mouse bitter receptor *Tas2r*138 as reported in the Supporting Information (Molecular Modeling section).

Molecular Docking. All docking experiments were carried out using the SeeSAR software package ver. 13.0.4 (BioSolveIT GmbH, St. Augustin, Germany)[19] by applying the integrated "binding site" computation and "docking" modules (more details in the Supporting Information, Molecular Docking section). The best docking solutions for each bitter compound and receptor were further visualized using Biovia Discovery Studio Visualizer 2024.[20]

Evaluation of Drug-Likeness. Physicochemical and drug-like properties of all ligands were predicted using SeeSAR ver. 13.0.4 (BioSolveIT GmbH, St. Augustin, Germany)[19] and DataWarrior ver. 5.5.0.[30]

■ ASSOCIATED CONTENT

Supporting Information

The Supporting Information is available free of charge at https://pubs.acs.org/doi/10.1021/acs.jnatprod.4c00532.

Molecular modeling and molecular docking protocols, characterization of compounds present in the ICE-4 mixture standard, UV−vis and LC-MS/MS spectra of hop extracts, Tas2r138 and T2R38 binding pocket,

https://doi.org/10.1021/acs.jnatprod.4c00532
J. Nat. Prod. 2024, 87, 2021−2033

hydrogen bonds and hydrophobic and electrostatic interaction of hop bitter molecules with the Tas2r138 (Q4VHE7.1.A) and T2R38 (P59533-F1) binding pocket, primer sequences for real-time PCR, primary amino acid sequence (331 aa) of the mouse taste receptor type 2 member 38 (Tas2r38), HPLC chromatogram of the ICE-4 standard at 325 nm in analytical mode, structural alignment of Tas2r138 and T2R38 bitter receptors and amino acids sequence alignment of Tas2r138 and T2R38, 3D and 2D representations of the interactions with the binding pocket of Tas2r138 (Q4VHE7.1.A), 3D and 2D representations of the interactions with the binding pocket of T2R38 (P59533-F1), and computed thermodynamic profiles obtained from hop molecules' best docking poses into Tas2r138 (model Q4VHE7.1.A) and T2R38 (model P59533-F1) (PDF)

AUTHOR INFORMATION

Corresponding Authors

Nikolay T. Tzvetkov − *Institute of Molecular Biology "Roumen Tsanev", Department of Biochemical Pharmacology & Drug Design, Bulgarian Academy of Sciences, 1113 Sofia, Bulgaria*; Phone: +359 2 979 2665; Email: ntzvetkov@bio21.bas.bg

Luigi Milella − *Department of Science, University of Basilicata, 85100 Potenza, Italy*; orcid.org/0000-0002-5874-1237; Phone: +39 0971 205525; Email: luigi.milella@unibas.it

Authors

Ludovica Lela − *Department of Science, University of Basilicata, 85100 Potenza, Italy*

Maria Ponticelli − *Department of Science, University of Basilicata, 85100 Potenza, Italy; Institute of Molecular Biology "Roumen Tsanev", Department of Biochemical Pharmacology & Drug Design, Bulgarian Academy of Sciences, 1113 Sofia, Bulgaria*

Vittorio Carlucci − *Department of Science, University of Basilicata, 85100 Potenza, Italy*

Jan F. Stevens − *Department of Chemistry and the Linus Pauling Institute, Oregon State University, Corvallis, Oregon 97331, United States; Department of Pharmaceutical Sciences, Oregon State University, Corvallis, Oregon 97331, United States*; orcid.org/0000-0002-6348-9347

Immacolata Faraone − *Department of Science, University of Basilicata, 85100 Potenza, Italy; Innovative Startup Farmis s.r.l., 85100 Potenza, Italy*

Complete contact information is available at: https://pubs.acs.org/10.1021/acs.jnatprod.4c00532

Author Contributions

[▽]L.L. and M.P. contributed equally to this work. L.L. and M.P.: *in vitro* and *in silico* experiments, data analysis, figure/table preparation, and manuscript draft. V.C. and I.F.: data analysis, chromatographic analysis. L.M., N.T.T, and J.F.S.: conceptualization, data analysis, experimental design, and manuscript reviewing and editing. L.M. funding

Notes

The authors declare no competing financial interest.

ACKNOWLEDGMENTS

Project SPIA-Valorization of byproducts from the agro-food chain CUP: G49J19001350004. DGR no. 527/2019 "PO FESR BASILICATA 2014-2020-Axis I-Research, Innovation Action and Technological Development-Action 1B.1.2.1-Avviso Pubblico per il sostegno alla creazione e sviluppo dei Cluster Tecnologici della Regione Basilicata e alla realizzazione di progetti di Ricerca e Sviluppo. Project FULLNESS no. F/200099/01-03/X45.

REFERENCES

(1) Su, Y.; Jie, H.; Zhu, Q.; Zhao, X.; Wang, Y.; Yin, H.; Kumar Mishra, S.; Li, D. *Biomed Res. Int.* **2019**, *2019*, 6301915.

(2) Descamps-Solà, M.; Vilalta, A.; Jalsevac, F.; Blay, M. T.; Rodríguez-Gallego, E.; Pinent, M.; Beltrán-Debón, R.; Terra, X.; Ardévol, A. *Front. Nutr.* **2023**, *10*, 1215889.

(3) Jaggupilli, A.; Singh, N.; Upadhyaya, J.; Sikarwar, A. S.; Arakawa, M.; Dakshinamurti, S.; Bhullar, R. P.; Duan, K.; Chelikani, P. *Mol. Cell. Biochem.* **2017**, *426*, 137−147.

(4) Jeruzal-Świątecka, J.; Fendler, W.; Pietruszewska, W. *Int. J. Mol. Sci.* **2020**, *21*, 5156.

(5) Depoortere, I. *Gut* **2014**, *63*, 179−190.

(6) Ponticelli, M.; Russo, D.; Faraone, I.; Sinisgalli, C.; Labanca, F.; Lela, L.; Milella, L. *Molecules* **2021**, *26*, 954.

(7) Bocquet, L.; Sahpaz, S.; Hilbert, J.; Rambaud, C.; Rivière, C. *Phytochem. Rev.* **2018**, *17*, 1047−1090.

(8) (a) Ramos, M. P.; Vilariño, J. M. L. *J. Inst. Brew.* **2023**, *129*, 97−109. (b) Dunkel, A.; Hofmann, T.; Di Pizio, A. *J. Agric. Food. Chem.* **2020**, *68*, 10414−10423.

(9) Intelmann, D.; Batram, C.; Kuhn, C.; Haseleu, G.; Meyerhof, W.; Hofmann, T. *Chemosens. Percept.* **2009**, *2*, 118−132.

(10) Kok, B. P.; Galmozzi, A.; Littlejohn, N. K.; Albert, V.; Godio, C.; Kim, W.; Kim, S. M.; Bland, J. S.; Grayson, N.; Fang, M.; et al. *Mol. Metab.* **2018**, *16*, 76−87.

(11) Yamazaki, T.; Morimoto-Kobayashi, Y.; Koizumi, K.; Takahashi, C.; Nakajima, S.; Kitao, S.; Taniguchi, Y.; Katayama, M.; Ogawa, Y. *J. Nutr. Biochem.* **2019**, *64*, 80−87.

(12) Bitarafan, V.; Fitzgerald, P. C.; Poppitt, S. D.; Ingram, J. R.; Feinle-Bisset, C. *Appetite* **2023**, *184*, No. 106490.

(13) Walker, E. G.; Lo, K. R.; Pahl, M. C.; Shin, H. S.; Lang, C.; Wohlers, M. W.; Poppitt, S. D.; Sutton, K. H.; Ingram, J. R. *Am. J. Clin. Nutr.* **2022**, *115*, 925−940.

(14) Chupeerach, C.; Tapanee, P.; On-Nom, N.; Temviriyanukul, P.; Chantong, B.; Reeder, N.; Adegoye, G. A.; Tolar-Peterson, T. *Biomedicine* **2021**, *11*, 43.

(15) Melis, M.; Errigo, A.; Crnjar, R.; Pes, G. M.; Tomassini Barbarossa, I. *Sci. Rep.* **2019**, *9*, 18047.

(16) Sternini, C. *American journal of physiology. Gastrointestinal and liver physiology* **2007**, *292*, G457−461.

(17) *AlphaFold*; EMBL-EBI: Cambridgeshire, U.K., n.d. https://alphafold.ebi.ac.uk/ (accessed 2024-01-15).

(18) Rarey, M.; Kramer, B.; Lengauer, T.; Klebe, G. *J. Mol. Biol.* **1996**, *261*, 470−489.

(19) *SeeSAR*, ver. 13.0.4; BioSolveIT GmbH: Sankt Augustin, Germany, 2023. https://www.biosolveit.de/SeeSAR/ (accessed 2024-01-02).

(20) *BioviaDiscoveryStudio*; Dassault Systemes: Vélizy-Villacoublay, France, n.d.https://www.3ds.com/ (accessed 2024-01-02).

(21) Rankovic, Z. *J. Med. Chem.* **2017**, *60*, 5943−5954.

(22) Clark, D. E. *J. Pharm. Sci.* **1999**, *88*, 807−814.

(23) Tzvetkov, N. T.; Antonov, L. *J. Enzyme Inhib. Med. Chem.* **2017**, *32*, 960−967.

(24) Freeman-Cook, K. D.; Hoffman, R. L.; Johnson, T. W. *Future Med. Chem.* **2013**, *5*, 113−115.

(25) Abad-Zapatero, C. *Expert Opin. Drug Discovery* **2007**, *2*, 469−488.

(26) Lipinski, C. A.; Lombardo, F.; Dominy, B. W.; Feeney, P. J. *Adv. Drug Delivery Rev.* **2012**, *64*, 4−17.
(27) Fernandes, J.; Gattass, C. R. *J. Med. Chem.* **2009**, *52*, 1214−1218.
(28) Azam, F.; Madi, A. M.; Ali, H. I. *J. Young Pharm.* **2012**, *4*, 184−192.
(29) Lapins, M.; Arvidsson, S.; Lampa, S.; Berg, A.; Schaal, W.; Alvarsson, J.; Spjuth, O. *J. Cheminform.* **2018**, *10*, 17.
(30) *DataWarrior*; openmolecules.org, n.d. https://openmolecules.org/datawarrior/ (accessed 2024-02-05).
(31) Wager, T. T.; Hou, X.; Verhoest, P. R.; Villalobos, A. *ACS Chem. Neurosci.* **2016**, *7*, 767−775.
(32) Tzvetkov, N. T.; Stammler, H.-G.; Hristova, S.; Atanasov, A. G.; Antonov, L. *Eur. J. Med. Chem.* **2019**, *162*, 793−809.
(33) Heffernan, S.; Nunn, L.; Harnedy-Rothwell, P. A.; Gite, S.; Whooley, J.; Giblin, L.; FitzGerald, R. J.; O'Brien, N. M. *Mar. Drugs* **2022**, *20*, 112.

https://doi.org/10.1021/acs.jnatprod.4c00532
J. Nat. Prod. 2024, 87, 2021−2033